Nonlinear Volume Holography for Wave-Front Engineering

Xu-Hao Hong,[1,2] Bo Yang,[1,3] Chao Zhang,[1,3,*] Yi-Qiang Qin,[1,3] and Yong-Yuan Zhu[1,2,†]
[1]*Key Laboratory of Modern Acoustics, National Laboratory of Solid State Microstructures and Collaborative Innovation Center of Advanced Microstructures, Nanjing University, Nanjing 210093, People's Republic of China*
[2]*School of Physics, Nanjing University, Nanjing 210093, China*
[3]*School of Modern Engineering and Applied Science, Nanjing University, Nanjing 210093, China*
(Received 1 January 2014; published 16 October 2014)

The concept of volume holography is applied to the design of an optical superlattice for the nonlinear harmonic generation. The generated harmonic wave can be considered as a holographic image caused by the incident fundamental wave. Compared with the conventional quasi-phase-matching method, this new method has significant advantages when applied to complicated nonlinear processes such as the nonlinear generation of special beams. As an example, we experimentally realized a second-harmonic Airy beam, and the results are found to agree well with numerical simulations.

DOI: 10.1103/PhysRevLett.113.163902 PACS numbers: 42.65.Ky, 42.40.-i

Nonlinear optics has been developed rapidly in recent decades, opening up new vistas in many classical fields. Because of the ability of generating special beams (such as nonlinear the Airy beam or vortex beam), the study on two-dimensional optical superlattices (OSL) with the quasi-phase-matching method has become a hot topic [1–10]. A reciprocal space phase-matching technique has been developed to deal with these new topics [11–14]. The key of this method contains two main parts, that is, the transverse axes forming a certain type of curved domain configuration for the phase modulation, and the propagation axis providing an appropriate poled period for compensating the phase mismatching. This technique, combined with the traditional quasi-phase-matching method and the wave-front engineering, has brought great possibilities to manipulate harmonics in many different fields [15–18].

The phase-matching problem can be also analyzed in real space. In our previous work, we developed a phase-matching technique to control the nonlinear wave front [19]. In this method, each area of the nonlinear medium is treated as a source of the nonlinear secondary wave, radiating harmonic waves outward, and the excited harmonic wave at a given area can be determined locally by the nonlinear coefficient and the fundamental wave (FW). The wave front at any position is related to the sum of the previously generated harmonic waves. Using this principle we have realized several nonlinear beam manipulations [19,20]. Furthermore, some nonlinear phenomenon such as the nonlinear Cherenkov radiation and the Raman-Nath diffraction [21–23] can be also well explained in this regard. However, this method also has its limitations. In some more complicated cases, such as nonlinear generation of special beams, this theory is found difficult to work with practically. Recently, a two-stage approach has been proposed which is able to transfer the fundamental wave into an arbitrary designed second-harmonic beam [24], but the wave-front shaping is performed by a linear optical process rather than a nonlinear process. And to date, none of the above wave-front engineering theories could provide a universal method to deal with arbitrary special beams all in the nonlinear regime. In this Letter, we show that this problem can be solved by introducing the nonlinear volume holography technique, which extends the concept of holography from linear optics to nonlinear optics.

Holography, being different from photography, is a technique that can store and reconstruct both the amplitude and phase of an object wave [25–29]. There are basically two categories of holography based on the difference of the recording medium: plane holography and volume holography. The volume holography not only inherits the specialty of the plane holography, but also has some additional features such as Bragg selectivity [30–33]. Conventionally, the holography is based on the interference fringes of the reference beam and the object beam recorded on a photographic film through corrugated surface gratings. Or in a photorefractive crystal the fringes can be imprinted as refractive index variation. Here, by transferring the fringes into the modulation of the nonlinear coefficient in a ferroelectric crystal, the nonlinear hologram can be realized.

Based on the secondary wave principle, in a second-harmonic generation (which acts as object beam) process the harmonic wave satisfies the brief expression $dE_{2\omega} \propto \chi^{(2)} E_\omega{}^2 dx$, here $\chi^{(2)}$ is the nonlinear coefficient. Considering the pump undepletion approximation and the plane wave form of FW, E_ω could be written as $E_\omega = A_\omega \exp(-ik_1 x)$, where k_1 is the wave vector of FW. Then the excited second-harmonic generation is depicted as follows:

$$dE_{2\omega} = C\chi^{(2)}A_{\omega}{}^2 \exp(-i2k_1x)dx \quad (1)$$

In this equation the initial phase $2k_1x$ can be considered as the spatial phase shift caused by a wave with the wave vector $2k_1$ before the excitation of the harmonic wave. In order to develop the nonlinear interference theory, a special light with wave vector of $2k_1$ and frequency of $\omega_2 = 2\omega_1$ should be introduced to interfere with the harmonic waves. It is interesting to find that the nonlinear polarization wave (NPW) meets all the demands. The NPW is generated by the FW, and then it radiates an optical field with the frequency doubled. For the sake of simplicity, here the NPW was set to be a plane wave [$\boldsymbol{E}_p = A_p \exp(-i2k_1x)$, which acts as the reference beam] and all the discussions are in a two dimensional system. By interfering with the NPW, the harmonic wave [$\boldsymbol{E}_h(x,y)$] can be stored in the form of interference fringe as Fig. 1(a) shows. The schematic diagram shows the general situation where the SH beam is noncollinear with the NPW. While in our experiment, we choose in-line (collinear) holography to generate the SH beam for the purpose of gaining higher nonlinear efficiency. The orange and green beams stand for the NPW and the harmonic wave, respectively, and they interfere with each other in the overlapped area to record both the amplitude and phase information of the harmonic wave. The light intensity distribution of the interference area is

$$\begin{aligned} I(x,y) &= |\boldsymbol{E}_p + \boldsymbol{E}_h|^2 \\ &= |\boldsymbol{E}_p|^2 + |\boldsymbol{E}_h|^2 + \boldsymbol{E}_p^* \cdot \boldsymbol{E}_h + \boldsymbol{E}_p \cdot \boldsymbol{E}_h^* \\ &= |\boldsymbol{E}_p|^2 + |\boldsymbol{E}_h|^2 + 2E_pE_h\cos\phi. \end{aligned} \quad (2)$$

Here ϕ is the phase difference between these two waves. It is worth noting that because of the law of energy conservation ($\omega_2 = 2\omega_1$), the interference pattern between the NPW and the harmonic wave is independent of the time.

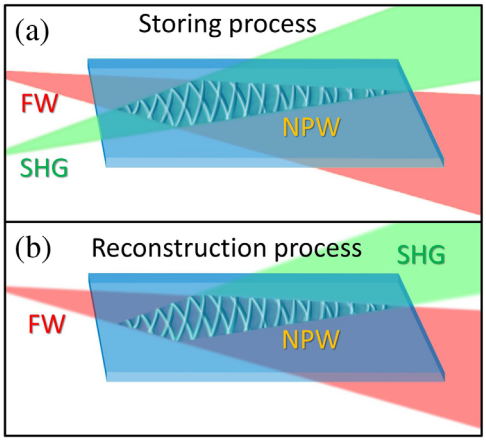

FIG. 1 (color online). Schematics of (a) the storing and (b) reconstruction processes in nonlinear volume holography.

That is to say the interference pattern in real space is stable without any beating frequency or vibration phenomenon.

Ignoring the background signal $I_0 = |\boldsymbol{E}_p|^2 + |\boldsymbol{E}_h|^2$, the normalized light field is $I' = \cos\phi$. Here the range of I' is between -1 and 1.

In order to record the "light distribution" into a nonlinear crystal as a hologram, the controllable quadratic nonlinear coefficient is introduced, which is defined as

$$\chi^{(2)} = d_{ij}\{I'\} \quad (3)$$

where d_{ij} is the element of the quadratic susceptibility used in the nonlinear process. In commonly used nonlinear crystal, the $\chi^{(2)}$ cannot be tuned in the full range from $-d_{ij}$ to d_{ij}. Taking the congruent lithium tantalate as an example, with the electric-field poling method only 180° antiparallel ferroelectric domain can be produced. The coefficient $\chi^{(2)}$ becomes binary format with two potential values only, either d_{ij} or $-d_{ij} = d_{ij} \cdot e^{i\pi}$. Thus, the structure function $f(x,y)$ (binary modulation function) required by nonlinear volume hologram can be simply determined by

$$f(x,y) = \mathrm{sgn}\{I'\}. \quad (4)$$

Considering that the binarization of the structure function might bring some error to the generated SH wave, we simulated the Airy beam generated in a binary structure and in an ideal continuous structure. The difference is small see [34]. In addition, there already exist some methods which can be used to mimic the structure function, such as the detour-phase encoding technique, where both the amplitude and phase information can be recorded by tuning the duty circle and the position of each domain [35].

The reconstruction process shown in Fig. 1(b) is the reverse process of the storing one. When the developed nonlinear hologram is illuminated by the FW (shown in red), the FW propagates through the hologram and excites harmonic waves (shown in green) with a different initial phase which is determined by the binary nonlinear optical coefficient. Then the harmonic waves diffract and interfere to form a certain pattern. The final field intensity E is equal to I' multiplied by the reference beam $\boldsymbol{E}_p$, giving

$$\boldsymbol{E} = \boldsymbol{E}_p\alpha(\boldsymbol{E}_p^*\boldsymbol{E}_h + \boldsymbol{E}_p\boldsymbol{E}_h^*) = \alpha|\boldsymbol{E}_p|^2\boldsymbol{E}_h + \alpha\boldsymbol{E}_p^2\boldsymbol{E}_h^* = \boldsymbol{E}' + \boldsymbol{E}'' \quad (5)$$

where α is a normalized coefficient. The first term $\boldsymbol{E}'$ is proportional to the initial SH wave $\boldsymbol{E}_h$, and the other is the phase-conjugated one which can be ignored. Except for a constant factor $\alpha|\boldsymbol{E}_p|^2$, the reconstructed wave $\boldsymbol{E}'$ is exactly the same as the expected harmonic wave $\boldsymbol{E}_h$.

In single sentences, the reference wave in nonlinear holography is the NPW, while the object wave is the SH

wave. The hologram pattern is determined by the interference fringe, and the reconstruction method is the reverse of the restoring process. For demonstration of the idea, we manipulated a wave with a complicated wave front, the Airy beam. According to Eq. (4), the OSL structure can be obtained as follows:

$$f(x,y) = \mathrm{sgn}\{\mathrm{Ai}[s-(2/\xi)^2]\exp[i\Delta k x + i(s\xi/2) - i(\xi^3/12)] + \mathrm{c.c.}\} \quad (6)$$

where Ai is the Airy function, $s = y/y_0$ represents a dimensionless traverse coordinate, y_0 is an arbitrary traverse scale, $\xi = x/k_2 y_0^2$ is a normalized propagation distance, and $\Delta k = k_2 - 2k_1$ is the wave vector mismatch in the second harmonic generation process [36,37].

We chose the $ee-e$ nonlinear process with the congruent $LiTaO_3$. In this case $d_{ij} = d_{33}$. The ones before the minus symbol represent the polarization of FW, after it represents the SH wave. Here the wavelengths of FW and the SH are 1064 and 532 nm, respectively, and T is set to be 150 °C to avoid the photorefractive effect and $y_0 = 20$ μm. The OSL structure thus designed is no longer periodic along the propagation direction. Because of the domain limitation in our traditional poling process (several microns), the beam "acceleration" cannot be set too large, otherwise the structure is too small to be fabricated. The numerical simulation of the SH field intensity distribution and the designed structure are shown in Figs. 2(a)–2(b).

The OSL structure was fabricated by two-dimensional poling of a 500 μm thick z-cut congruent lithium tantalate and then the x faces were polished. The length of the sample is 2 cm. Figure 2(c) shows the optical microscopic image of the sample surface after HF acid etching. Because of the practical poling technique, the duty cycle of the experimental structure is different from the calculated one. However, it will only lead to a slight loss to the conversion efficiency of the SH wave. Figure 3(a) shows the experimental layout. In the experiment a cw laser (LE-LS-1064-500TA) was used with the wavelength 1064 nm. An Airy beam was generated at the second-harmonic frequency. The power of FW was fixed at 500 mW with the peak intensity about 50 W/cm^2 and 1 mm beam diameter. There was no other optical element between the laser and the sample. A filter was fixed closely to the sample to block the infrared light while transmitting the green harmonic wave. The spacing between Airy lobes was designed to be dozens of microns. In order to amplify the details of Airy lobes, an imaging system (including lens, screen, and a camera) was used. The distance between the lens and the screen (image distance) was set at 500 mm, which is more than 16 times longer than the focal length (30 mm). Calculated by the lens imaging formula, the projection on the screen was the real image of the beam cross profile at the position of 32 mm (the distance between the object plane and the lens). Figure 3(a) shows the imaging system, which is inside the dashed box. When moving the entire imaging system the distances of each element are kept constant. Figure 3(b) shows a series of the photographs with spacing of 40 mm to display the Airy beam's most exotic features. It exhibits the propagation dynamics of a typical Airy beam which is nondiffraction and acceleration forming a parabolic arc.

To illustrate the self-healing character, a needle was inserted into the light path in the experiment and it blocks the second and the third lobes [the dashed curve in Fig. 3

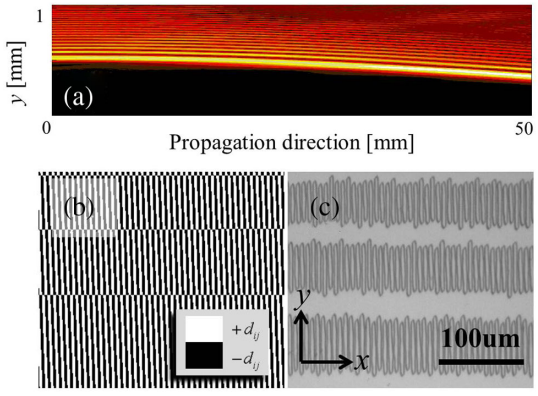

FIG. 2 (color online). (a) Numerical simulation of a propagation nonlinear Airy beam. (b) Calculated and (c) optical microscopic images of OSL.

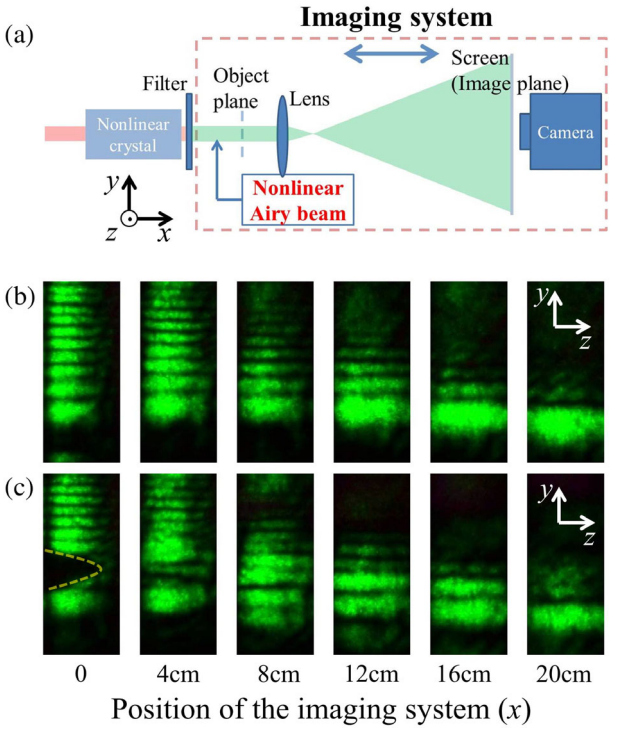

FIG. 3 (color online). (a) Experimental setup for the generation of the nonlinear Airy beam. The imaging system is moving along the x axis during the measurement. (b) Transverse patterns of the generated Airy beam and (c) the self-healing property of the nonlinear Airy beam.

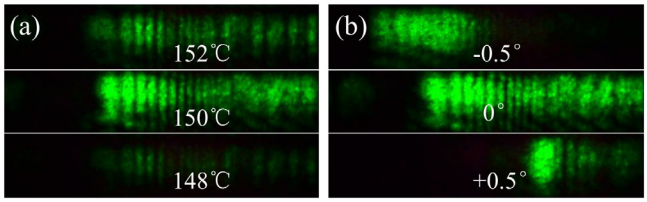

FIG. 4 (color online). Transverse patterns showing (a) temperature selectivity and (b) angular selectivity of the nonlinear volume holography.

(c)]. Likewise, photographs were shot and the propagation trajectory is shown in this figure. Using the imaging system, the light distribution nearby the obstacle has been detected. At the position of $x = 40$ mm the lost lobes start to reappear, and at about $x = 80$ mm the image recovers the normal Airy wave profile [shown in Fig. 3(c)]. However, some weak diffraction light was inevitably generated below the main lobe.

Just like the linear volume holography, there are also strong wavelength, temperature, and angular selectivities in the nonlinear volume holography. For example, the temperature and angular dependence properties in the experiment are shown in Figs. 4(a) and 4(b), respectively. When the temperature was shifted 2 ℃ away from 150 ℃, the main lobe of the Airy beam disappeared and the cross profile no longer kept the Airy beam wave profile. Likewise, when the incidence angle varied 0.5°, the SH distribution changed significantly. These selectivities impose restrictions on the light path, that is, no optical element is needed to be inserted between the laser and the sample, thus avoiding the distortion of the FW.

The method can be even applied to the case where the harmonic wave doesn't have an analytical form. In this situation, in order to engineer the wave front of an arbitrary harmonic wave in far field, the Fresnel diffraction formula should be adopted to calculate the propagation field in the recording area (interference region):

$$E_h(x,y) = \frac{C}{\sqrt{\lambda x}} \exp(ikx) \int_{-\infty}^{\infty} E_h(0,y_0) \exp\left[i\frac{k}{2x}(y-y_0)^2\right] dy_0. \tag{7}$$

Using this equation, we can numerically calculate the field distribution $E_h(x,y)$ provided that the initial wave front $E_h(x,y)|_{x=0}$ is given; thus, the required OSL structure can be designed accordingly by inserting the calculated field distribution E_h into Eqs. (2) and (4).

It is interesting to compare the present work with the approach used in Ref. [11], which is more similar to the Fourier holography, while our method belongs to the Fresnel holography. The Fourier holography deals with the wave information in the reciprocal space. Since no lens is needed to realize the optical Fourier transform in the reconstruction process, the nonlinear Fresnel holography might be more useful than the Fourier holography for nanophotonics and integrated photonics where a smaller and more compact device is preferred.

In conclusion, by introducing the concept of volume holography into the nonlinear optics we have developed a new method for nonlinear wave-front engineering. It has significant advantages when dealing with complicated nonlinear generation processes involving special beams [34]. As a demonstration, we have experimentally generated a second-harmonic Airy beam. The method is universal and could be applied to other nonlinear optical processes. In principle, it might even be applied to some nonoptical processes that require complicated wave-front modulation, such as the Airy beam generation of surface plasmon polaritons and electron beams.

This work is supported by the State Key Program for Basic Research of China (Grant No. 2010CB630703), the National Natural Science Foundation of China (Grants No. 11374150, No. 11074120, No. 11274163, and No. 11274164) and Priority Academic Program Development of Jiangsu Higher Education Institutions of China (PAPD).

*Corresponding author.
zhch@nju.edu.cn
†Corresponding author.
yyzhu@nju.edu.cn

[1] V. Berger, Phys. Rev. Lett. **81**, 4136 (1998).
[2] Y. Zhang, J. M. Wen, S. N. Zhu, and M. Xiao, Phys. Rev. Lett. **104**, 183901 (2010).
[3] J. M. Wen, Y. Zhang, S. N. Zhu, and M. Xiao, J. Opt. Soc. Am. B **28**, 275 (2011).
[4] N. G. R. Broderick, G. W. Ross, H. L. Offerhaus, D. J. Richardson, and D. C. Hanna, Phys. Rev. Lett. **84**, 4345 (2000).
[5] J. R. Kurz, A. M. Schober, D. S. Hum, A. J. Saltzman, and M. M. Fejer, IEEE J. Sel. Top. Quantum Electron. **8**, 660 (2002).
[6] J. J. Chen and X. F. Chen, Phys. Rev. A **80**, 013801 (2009).
[7] A. Arie and N. Voloch, Laser Photonics Rev. **4**, 355 (2010).
[8] P. Zhang, Y. Hu, D. Cannan, A. Salandrino, T. C. Li, R. Morandotti, X. Zhang, and Z. G. Chen, Opt. Lett. **37**, 2820 (2012).
[9] P. Zhang, Y. Hu, T. C. Li, D. Cannan, X. B. Yin, R. Morandotti, Z. G. Chen, and X. Zhang, Phys. Rev. Lett. **109**, 193901 (2012).
[10] N. V. Bloch, K. Shemer, A. Shapira, R. Shiloh, I. Juwiler, and A. Arie, Phys. Rev. Lett. **108**, 233902 (2012).
[11] T. Ellenbogen, N. V. Bloch, A. G. Padowicz, and A. Arie, Nat. Photonics **3**, 395 (2009).
[12] I. Doleva and A. Arie, Appl. Phys. Lett. **97**, 171102 (2010).
[13] A. Shapira, I. Juwiler, and A. Arie, Opt. Lett. **36**, 3015 (2011).
[14] A. Shapira, R. Shiloh, I. Juwiler, and A. Arie, Opt. Lett. **37**, 2136 (2012).

[15] L. Li, T. Li, S. M. Wang, C. Zhang, and S. N. Zhu, Phys. Rev. Lett. **107**, 126804 (2011).
[16] I. Dolev, I. Epstein, and A. Arie, Phys. Rev. Lett. **109**, 203903 (2012).
[17] L. Li, T. Li, S. M. Wang, and S. N. Zhu, Phys. Rev. Lett. **110**, 046807 (2013).
[18] N. V. Bloch, Y. Lereah, Y. Lilach, A. Gover, and A. Arie, Nature (London) **494**, 331 (2013).
[19] Y. Q. Qin, C. Zhang, Y. Y. Zhu, X. P. Hu, and G. Zhao, Phys. Rev. Lett. **100**, 063902 (2008).
[20] X. H. Hong, B. Yang, D. Zhu, C. Zhang, H. Huang, Y. Q. Qin, and Y. Y. Zhu, Opt. Lett. **38**, 1793 (2013).
[21] S. M. Saltiel, Y. Sheng, N. Bloch, D. N. Neshev, W. Krolikowski, A. Arie, K. Koynov, and Y. S. Kivshar, IEEE J. Quantum Electron. **45**, 1465 (2009).
[22] Y. Zhang, Z. D. Gao, Z. Qi, S. N. Zhu, and N. B. Ming, Phys. Rev. Lett. **100**, 163904 (2008).
[23] Y. Sheng, W. Wang, R. Shiloh, V. Roppo, A. Arie, and W. Krolikowski, Opt. Lett. **36**, 3266 (2011).
[24] A. Shapira, A. Libster, Y. Lilach, and A. Arie, Opt. Commun. **300**, 244 (2013).
[25] D. Gabor, Nature (London) **161**, 777 (1948).
[26] T. Dresel, M. Beyerlein, and J. Schwider, Appl. Opt. **35**, 6865 (1996).
[27] T. Dresel, M. Beyerlein, and J. Schwider, Appl. Opt. **35**, 4615 (1996).
[28] D. N. Christodoulides and T. H. Coskun, Opt. Lett. **21**, 1460 (1996).
[29] E. N. Leith and J. Upatnieks, J. Opt. Soc. Am. **52**, 1123 (1962).
[30] G. A. Rakuljic, V. Leyva, and A. Yariv, Opt. Lett. **17**, 1471 (1992).
[31] M. C. Bashaw, J. F. Heanue, A. Aharoni, J. F. Walkup, and L. Hesselink, J. Opt. Soc. Am. B **11**, 1820 (1994).
[32] G. A. Rakuljic and V. Leyva, Opt. Lett. **18**, 459 (1993).
[33] F. H. Mok, Opt. Lett. **18**, 915 (1993).
[34] See Supplemental Material at http://link.aps.org/supplemental/10.1103/PhysRevLett.113.163902 for more examples and analysis.
[35] A. W. Lohmann and D. P. Paris, Appl. Opt. **6**, 1739 (1967).
[36] M. V. Berry and N. L. Balazs, Am. J. Phys. **47**, 264 (1979).
[37] G. A. Siviloglou, J. Broky, A. Dogariu, and D. N. Christodoulides, Phys. Rev. Lett. **99**, 213901 (2007).